Neuron, Vol. 15, 941–949, October, 1995, Copyright © 1995 by Cell Press

An Inhibitor of the Kv2.1 Potassium Channel Isolated from the Venom of a Chilean Tarantula

Kenton J. Swartz and Roderick MacKinnon
Department of Neurobiology
Harvard Medical School
Boston, Massachusetts 02115

Summary

The Kv2.1 voltage-activated K^+ channel, a *Shab*-related K^+ channel isolated from rat brain, is insensitive to previously identified peptide inhibitors. We have isolated two peptides from the venom of a Chilean tarantula, G. spatulata, that inhibit the Kv2.1 K^+ channel. The two peptides, hanatoxin$_1$ ($HaTx_1$) and hanatoxin$_2$ ($HaTx_2$), are unrelated in primary sequence to other K^+ channel inhibitors. The activity of HaTx was verified by synthesizing it in a bacterial expression system. The concentration dependence for both the degree of inhibition at equilibrium (K_d = 42 nM) and the kinetics of inhibition ($k_{on} = 3.7 \times 10^4\ M^{-1}s^{-1}$; $k_{off} = 1.3 \times 10^{-3}\ s^{-1}$), are consistent with a bimolecular reaction between HaTx and the Kv2.1 K^+ channel. *Shaker*-related, *Shaw*-related, and *eag* K^+ channels were relatively insensitive to HaTx, whereas a *Shal*-related K^+ channel was sensitive. Regions outside the scorpion toxin binding site (S5-S6 linker) determine sensitivity to HaTx. HaTx introduces a new class of K^+ channel inhibitors that will be useful probes for studying K^+ channel structure and function.

Introduction

Peptide inhibitors provide valuable tools for probing the structure and function of ion channels. For example, scorpion toxins that were known to inhibit K^+ channels by occluding the pore (MacKinnon and Miller, 1988; Miller, 1988; Park and Miller, 1992) led to the identification of the pore-forming region (P region) of the channel protein (MacKinnon and Miller, 1989; MacKinnon et al., 1990; Hartmann et al., 1991; Yellen et al., 1991; Yool and Schwarz, 1991) and are being used to measure the dimensions of the outer pore mouth (Goldstein et al., 1994; Stampe et al., 1994; Stocker and Miller, 1994; Hidalgo and MacKinnon, 1995). These K^+ channel inhibitors also led to the determination of the subunit stoichiometry (MacKinnon, 1991) and the functional stoichiometry of inactivation gates (MacKinnon et al., 1993) in the *Shaker* K^+ channel. A further important application of peptide inhibitors has been to examine the localization and physiological roles of individual channel subtypes (e.g., Robitaille et al., 1993; Reger and Mintz, 1994).

A large number of K^+ channel inhibitors have been previously isolated from venomous animals (Haux et al., 1967; Shipolini et al., 1967; Billingham et al., 1973; Harvey and Karlsson, 1980; Possani et al., 1982; Miller et al., 1985; Halliwell et al., 1986; Penner et al., 1986; Smith et al., 1986; Stansfeld et al., 1986; Carbone et al., 1987; Chicchi et al., 1988; Lucchesi et al., 1989; Galvez et al., 1990; Crest et al., 1992; Garcia-Calvo et al., 1993; Werkman et al., 1993; Garcia et al., 1994). These inhibitors primarily target either the *Shaker*-related subfamily of voltage activated K^+ channels or the Ca^{2+}-activated K^+ channels. The four other subfamilies of voltage-activated K^+ channels (*Shab*-related, *Shaw*-related, *Shal*-related, and *eag*-related) and the inward rectifier K^+ channels are relatively insensitive to these toxins (Garcia et al., 1994; Grissmer et al., 1994; unpublished data). We set out to isolate inhibitors of the Kv2.1 K^+ channel (drk1; Frech et al., 1989), a *Shab*-related K^+ channel that is insensitive to the known high affinity inhibitors from scorpions and snakes (Garcia et al., 1994; unpublished data) and is prevalent in the mammalian nervous system (Trimmer, 1991; Hwang et al., 1993). Here, we describe the purification, synthesis, and initial characterization of a peptide inhibitor of the Kv2.1 K^+ channel.

Results

Purification of Kv2.1 K^+ Channel Inhibitors

The venom from Grammostola spatulata, a Chilean tarantula, produced particularly robust inhibition of the Kv2.1 K^+ channel. The Kv2.1 K^+ channel was expressed in Xenopus oocytes and studied using a two-electrode voltage clamp. Figure 1 shows that a 1:100 dilution of crude venom produced complete and reversible inhibition of K^+ current elicited by depolarization to 0 mV. After removal of venom from the recording chamber, the K^+ current recovered along a multiexponential time course, suggesting the existence of multiple inhibitors.

We fractionated G. spatulata venom using reverse-phase high performance liquid chromatography (HPLC) and tested individual peaks for activity against the Kv2.1 K^+ channel. Figures 2A and 2B show two sequential HPLC steps that allowed the purification of two peptide inhibitors of the Kv2.1 channel. The purified material, which we named hanatoxin (HaTx), had a characteristic elution profile, in that it always eluted in two peaks; the second, and predominant, peak is about 10-fold larger than the first (Figure 2C). Collection and reinjection of each individual peak again gave two peaks with the same retention times and in the same ratio as shown in Figure 2C. We conclude that the two peaks of native HaTx have the same chemical composition; i.e., the two peaks are a chromatographic phenomenon.

Reduction of HaTx with 10–50 mM dithiothreitol gave two peaks of roughly equal height with retention times that were longer than those observed for the folded, active material (Figure 2D). This suggested the existence of two distinct peptides that were not resolved in the folded state. The two peaks observed under reducing conditions, designated $HaTx_1$ and $HaTx_2$, had molecular weights of 4117 and 4102 KDa, respectively, when analyzed by mass spec-

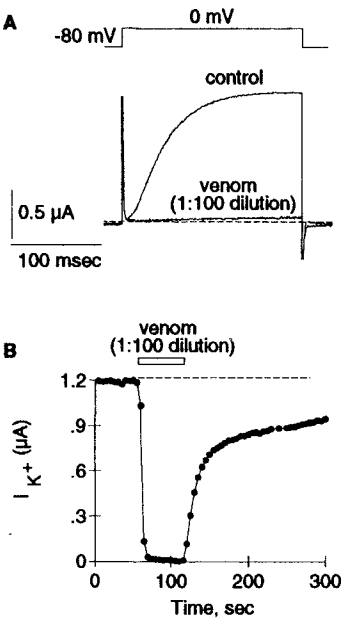

Figure 1. Inhibition of the Kv2.1 K^+ Channel by Grammostola spatulata Venom

(A) Effects of a 1:100 dilution of venom on the Kv2.1 K^+ channel expressed in Xenopus oocytes. K^+ currents were elicited by depolarization to 0 mV from a holding potential of -80 mV. Traces are shown without leak subtraction.

(B) Steady-state K^+ currents measured 200 ms after depolarization to 0 mV are shown plotted as a function of time. Currents were elicited at 5 s intervals.

trometry. Amino acid sequencing showed that the two isoforms of HaTx differed only at residue 13 (Figure 3), where $HaTx_1$ contained Ser and $HaTx_2$ contained Ala. The molecular weights predicted from sequence analysis were 4119 KDa for $HaTx_1$ and 4103 KDa for $HaTx_2$, consistent with those directly determined by mass spectrometry. The HaTxs contain 6 cysteines, 6 basic residues (Lys or Arg), and 4 acidic residues (Glu or Asp). They also contain a large number of hydrophobic residues (4 Phe, 2 Tyr, 1 Trp, 2 Leu). Amino acid analysis was consistent with the sequence shown in Figure 3 (Table 1).

Figures 2E and 2F show the inhibitory effect of native HaTx (a mixture of the two isoforms) on the Kv2.1 K^+ channel. The channel was activated by depolarizing steps to 0 mV from a holding potential of −80 mV, elicited every 20 s. External application of 200 nM HaTx reversibly inhibited voltage-activated K^+ current in oocytes expressing the Kv2.1 channel by ~ 77%. Both the onset and recovery from inhibition were slow; single exponential fits to the data in Figure 2F gave time constants of 114 s (onset) and 828 s (recovery).

Production of Recombinant Hanatoxin

We produced recombinant HaTx in order to verify that this peptide was indeed the inhibitory component in the spider venom. $HaTx_1$ was produced as a fusion with maltose binding protein (malE) in E. coli (Riggs, 1994), with a Met residue present just before the N terminal Glu of HaTx (Figure 4A). The fusion protein was reacted with cyanogen bromide (which cleaves the peptide bond after Met; Gross and Witkop, 1962) following its isolation from the periplasmic space of E. coli. Figure 4B shows an HPLC chromatogram of the cyanogen bromide cleavage products. The majority of the peaks shown are different folds of $HaTx_1$. One peak eluting at 51 min coelutes with native HaTx and inhibits the Kv2.1 K^+ channel (Figures 4C and 4D). For the oocyte shown in Figures 4C and 4D, 100 nM recombinant $HaTx_1$ inhibited K^+ channel current by 55%, in close agreement with the inhibition seen with native HaTx (see Figures 2 and 5). Furthermore, the kinetics of inhibition by recombinant $HaTx_1$ were in reasonable agreement with that observed for native HaTx. We conclude that HaTx is an inhibitor of the Kv2.1 K^+ channel. Inefficiencies in both the cyanogen bromide cleavage reaction (10–20%) and the folding of HaTx (~1%) contribute to produce very low yields of recombinant $HaTx_1$. In subsequent studies, we therefore used native HaTx. While this is a mixture of two isoforms, we know that these two isoforms differ by only a single amino acid and that recombinant $HaTx_1$ has comparable affinity and kinetics when compared to the native material.

Functional Characterization of Hanatoxin

The concentration dependence for the fractional inhibition at equilibrium is plotted in Figure 5. The data for HaTx-induced inhibition could be well fit by an equation for 1:1 binding between HaTx and the Kv2.1 channel with an equilibrium dissociation constant (K_d) of 42 nM.

Kinetic studies for HaTx-induced inhibition of the Kv2.1 channel are shown in Figure 6. The kinetics of HaTx-induced inhibition were consistent with a bimolecular reaction between HaTx and the Kv2.1 K^+ channel: $1/\tau$ for onset of inhibition varied linearly with HaTx concentration, while $1/\tau$ for recovery from inhibition was independent of HaTx concentration (Figures 6A and 6B). The rate constants calculated from these data ($k_{on} = 3.7 \times 10^4\ M^{-1}s^{-1}$; $k_{off} = 1.3 \times 10^{-3}\ s^{-1}$) indicate that both association and dissociation of HaTx is very slow. The association rate constant for HaTx is about 1000-fold slower than that of charybdotoxin or agitoxin$_2$ for the various K^+ channels (Anderson et al., 1988; Goldstein et al., 1994; Gross et al., 1994). The K_d calculated from the ratio of k_{off}/k_{on} (35 nM) compares reasonably well to that obtained from the concentration dependence of inhibition at equilibrium (42 nM).

Specificity of Hanatoxin

We screened a variety of other voltage-activated K^+ channels for sensitivity to HaTx, and the results are shown in Figure 7 (for nomenclature, see Gutman and Chandy, 1993). The *Shaker* K^+ channel (Kamb et al., 1988) and a number of its mammalian homologs were relatively insensitive to HaTx. Kv1.1 (Stühmer et al., 1989), Kv1.3 (Swanson et al., 1990), and Kv1.6 (Swanson et al., 1990) were not inhibited by 500 nM HaTx, while the *Shaker* K^+ channel was only weakly inhibited. Kv3.1 (Grissmer et al., 1992), a *Shaw*-related K^+ channel and the *eag* K^+ channel (Warmke et al., 1991), were also insensitive to 500 nM HaTx. Interestingly, the Kv4.2 channel (Baldwin et al., 1991), a

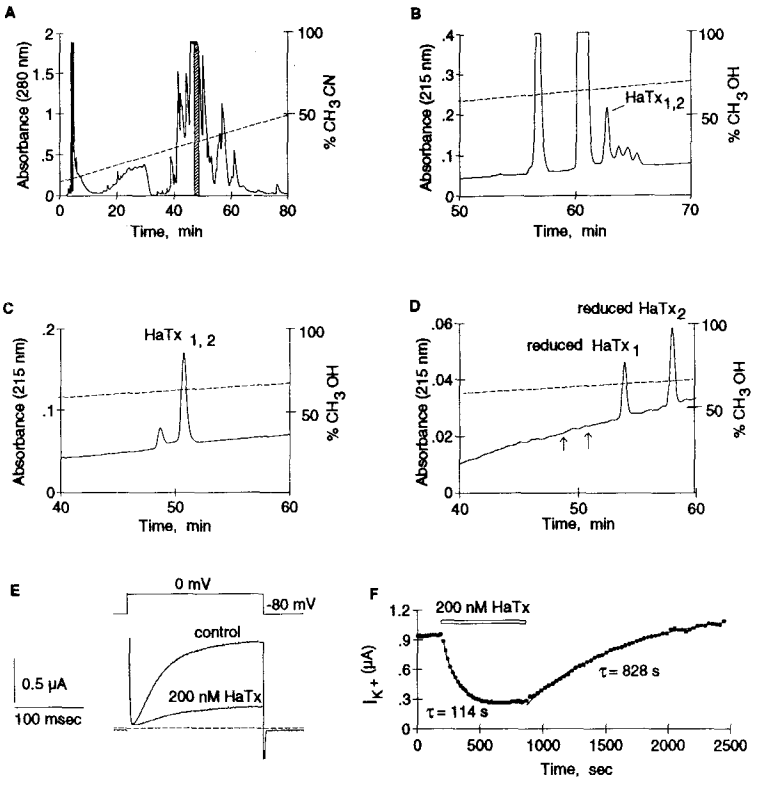

Figure 2. Purification of Hanatoxin from G. spatulata Venom

(A) Reverse-phase HPLC chromatogram illustrating the first step in the purification of HaTx from 100 μl of venom. The first step employed a linear gradient from 10% to 50% mobile phase B over 80 min, where mobile phase A was 0.1% trifluoroacetic acid (TFA) in water, and mobile phase B was 0.08% TFA in acetonitrile. The fraction indicated by the shaded region produced the largest fractional inhibition of Kv2.1 with the slowest recovery from inhibition ($\tau_{off} \approx$ 500–800 s).

(B) Reverse-phase HPLC chromatogram illustrating a second purification step using a linear gradient from 0% to 100% mobile phase B over 80 min, where mobile phase A was 0.1% TFA, 25% methanol in water; and mobile phase B was 0.08% TFA, 75% methanol in water. Two peaks in this run were active against the Kv2.1 channel. The peak labeled $HaTx_{1,2}$ inhibited Kv2.1 with slow recovery ($\tau_{off} \approx$ 750 s), while the large preceding peak inhibited the channel with relatively fast recovery ($\tau_{off} \approx$ 50 s).

(C) Reverse-phase HPLC chromatogram of purified HaTx. This chromatogram was obtained under similar conditions as in B, except that the gradient was from 25% to 100% mobile phase B over 80 min. The two peaks seen in this run represent a characteristic elution profile of HaTx. Either peak regenerates the same two peaks when reinjected.

(D) Reverse-phase HPLC chromatogram showing separation of the two isoforms of HaTx following reduction with 10 mM dithiothreitol. Gradient and solvents conditions are identical to those described above for (C). The molecular weight of the peak labeled $HaTx_1$ was 4117 KDa and the molecular weight of the peak labeled $HaTx_2$ was 4102 KDa. The ratio of these two isoforms varied somewhat between different batches of venom (from 1:1.5 to 1:0.65).

(E and F) Effects of native HaTx on the Kv2.1 K+ channel expressed in Xenopus oocytes. K+ currents shown in E were elicited by depolarization to 0 mV from a holding potential of -80 mV. Traces are shown without leak subtraction. In (F), the K+ currents measured 200 ms after depolarization to 0 mV are plotted as a function of time. Single exponential fits (least squares; solid curves) for both onset of, and recovery from, HaTx-induced inhibition are superimposed on the data points.

Shal-related K+ channel, was sensitive to HaTx (Figure 7). One interesting feature of HaTx-induced inhibition is the recovery from inhibition during a depolarizing pulse. This behavior, which is obvious in the *Shaker* and Kv4.2 K+ channel recordings, can also be observed in Kv2.1 when the blocked and unblocked records are scaled and superimposed (see Discussion).

Regions outside the S5-S6 Linker Determine Sensitivity to Hanatoxin

The S5-S6 linker forms the binding site for K+ channel inhibitors such as charybdotoxin, agitoxin (AgTx), and dendrotoxin (MacKinnon and Miller, 1989; Hurst et al., 1991; Stocker et al., 1991; Garcia et al., 1994). To test whether the same region is important for inhibition by HaTx, we constructed a chimera between Kv2.1 and the *Shaker* K+ channel (Figure 8A). The Kv2.1 K+ channel is sensitive to HaTx but not to $AgTx_2$, whereas the *Shaker* K+ channel is very sensitive to $AgTx_2$ but not to HaTx (Garcia et al., 1994). When the S5-S6 linker from Kv2.1 is transferred to the *Shaker* channel, $AgTx_2$ sensitivity is lost (Figure 8B), as expected from previous work (e.g., Gross et al., 1994). However, HaTx sensitivity is not acquired, and furthermore, the weak inhibition of the *Shaker* channel by HaTx is unaffected by the mutation (Figure 8B). These results imply that HaTx interacts with a region of K+ channels outside the S5-S6 linker.

	1 10 20 30
Hanatoxin$_1$ (HaTx$_1$)	ECRYLFGGCKTTSDCCKHLGCK FRDKY CAWDFTFS
Hanatoxin$_2$ (HaTx$_2$)	----------A--------- ----- --------
Grammotoxin	D-VRFW-K-SQ-----P--A--SKWPRNI-V--GSV

Figure 3. Amino Acid Sequence of Hanatoxins

Amino acid sequence for the two isoforms of HaTx and grammotoxin. Dashes in the sequence of $HaTx_2$ and grammotoxin indicate identity with $HaTx_1$. Two single residue gaps have been introduced in the sequence of $HaTx_1$ and $HaTx_2$ for comparison with grammotoxin. The sequence of grammotoxin is from Lampe et al., 1993.

Discussion

Three main categories of peptide inhibitors of K+ channels have been described thus far. While this classification is based on comparison of different amino acid sequences and three-dimensional structures, it ultimately reflects the animal (scorpion, snake, or bee) from which the inhibitors were isolated. Many different K+ channel inhibitors have been isolated from scorpion venom; they are similar in

Table 1. Amino Acid Analysis of Native Hanatoxin

Amino Acid	Residues Per Molecule	
	Observed	Theoretical
Asp/Asn	3.1	3
Glu/Gln	1.2	1
Ser	1.6	1.5*
Gly	3.2	3
His	0.9	1
Arg	2.1	2
Thr	2.7	3
Ala	1.4	1.5*
Pro	0.0	0
Tyr	1.7	2
Val	0.1	0
Met	0.1	0
Iso	0.1	0
Leu	2.0	2
Phe	3.8	4
Lys	3.9	4

*The expected composition of 1.5 for Ser and Ala reflects the fact that amino acid analysis was done on a mixture of the two isoforms of HaTx and that their relative abundance in the mixture is approximately equal. Cysteine residues were not derivatized for this analysis and therefore were not detected.

sequence (Possani et al., 1982; Miller et al., 1985; Smith et al., 1986; Chicchi et al., 1988; Lucchesi et al., 1989; Galvez et al., 1990; Crest et al., 1992; Garcia-Calvo et al., 1993; Garcia et al., 1994) and structure (Lambert et al., 1990; Bontems et al., 1991a, 1991b,; Johnson and Sugg, 1992; Krezel et al., 1995). Six dendrotoxin isoforms have been isolated from the venom of Dendroaspis snakes (Strydom, 1972, 1973; Harvey and Karlsson, 1980; Joubert and Taljaard, 1980; Harvey and Anderson, 1985; Benishin et al., 1988). The three-dimensional structures of α-dendrotoxin and dendrotoxin-I have been recently solved (Skarzynski, 1992; Foray et al., 1993). Bee venom has provided us with apamin (Haux et al., 1967; Shipolini et al., 1967; Pease and Wemmer, 1988) and mast cell degranulating peptide (MCDP; Billingham et al., 1973; Kumar et al., 1988). HaTx, isolated from a spider venom, represents a new category of K^+ channel inhibitors. Its amino acid sequence and spacing of 6 cysteine residues clearly distinguishes HaTx from the previously described K^+ channel inhibitors.

Although a complete pharmacological characterization of the many different cloned K^+ channels has yet to be done, several patterns are emerging. For instance, the inhibitors from scorpions, snakes, and bees appear to target primarily either the *Shaker*-related subfamily of voltage-activated K^+ channels or the Ca^{2+}-activated K^+ channels (e.g., Blatz and Magleby, 1986; Stühmer et al., 1989; Swanson et al., 1990; Kirsch et al., 1991; Stocker et al., 1991; Crest et al., 1992; Garcia-Calvo et al., 1993; Garcia et al., 1994; Grissmer et al., 1994). The *Shab*-related (Kv2-like), *Shaw*-related (Kv3-like), *Shal*-related (Kv4-like), *eag*-related, and inward rectifier K^+ channels are relatively insensitive to these toxins (Garcia et al., 1994; Grissmer et al., 1994; unpublished data). HaTx targets the Kv2 and Kv4 K^+ channels and therefore opens new avenues for studying these channels. It should allow us to understand the physiological roles of these channels in different cells. Also, mapping the HaTx binding site, as has already been done for some scorpion toxins, will hopefully reveal new structural features of K^+ channels (see below).

A common mechanism by which peptides inhibit ion channels is to prevent K^+ conduction by binding to the outer mouth and occluding the pore. This mechanism is best demonstrated for the K^+ channel inhibitors from scorpions (MacKinnon and Miller, 1988, 1989; Miller, 1988; Park and Miller, 1992). Dendrotoxin probably works through a similar mechanism, since residues in the S5-S6 linker (which contains the pore-forming region) are critical determinants of toxin blockade (Hurst et al., 1991; Stocker et al., 1991). Apamin and MCDP have not been studied

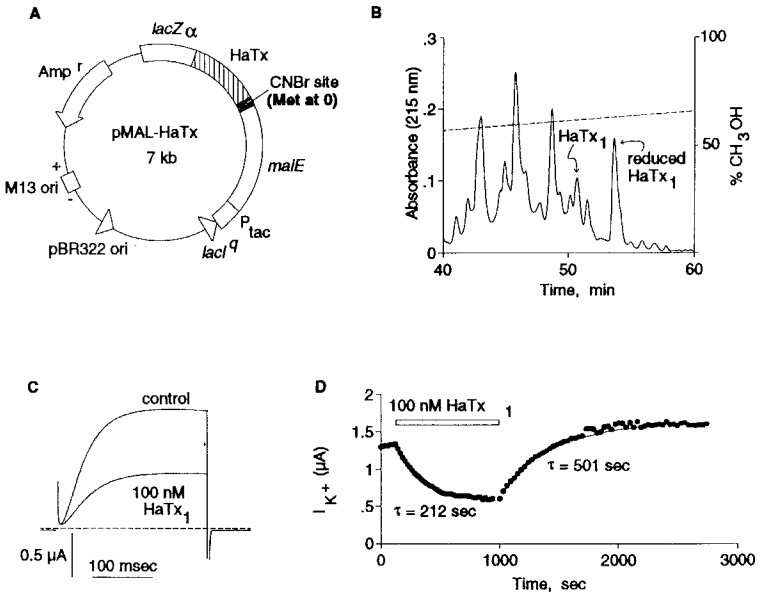

Figure 4. Production and Characterization of Recombinant Hanatoxin$_1$

(A) Plasmid construct containing HaTx$_1$ as a translational fusion with maltose binding protein (malE).

(B) Reverse-phase HPLC chromatogram illustrating the separation of different folds of HaTx$_1$ following cleavage from malE with cyanogen bromide. The peak labeled HaTx$_1$ coelutes with native HaTx. Reduction of this material with 10 mM dithiothreitol yields one major peak coeluting with reduced native HaTx$_1$ (see Figure 2D).

(C and D) Inhibition by HaTx$_1$ of the Kv2.1 K^+ channel expressed in Xenopus oocytes. K^+ currents shown in (C) were elicited by depolarization to 0 mV from a holding potential of −80 mV. Traces are shown without leak subtraction. In (D), the steady-state K^+ currents measured 250 ms after depolarization to 0 mV are plotted as a function of time. Single exponential fits (least squares; solid curves) for both onset of, and recovery from, HaTx$_1$-induced inhibition are superimposed on the data points.

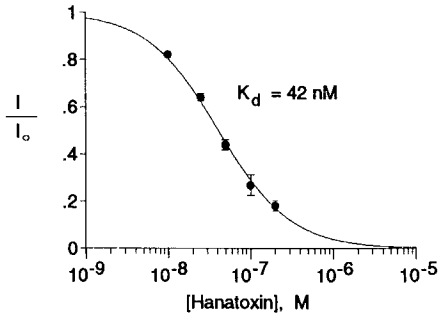

Figure 5. Concentration Dependence of Hanatoxin-Induced Inhibition

Plot of the fraction of unblocked current as a function of HaTx concentration. Each point is the mean ± SEM for 3–4 different oocytes. The smooth curve is a fit of $I/I_o = \{1 + ([HaTx]/K_d)\}^{-1}$, where I is the current in the presence of HaTx and I_o is the control current, both measured at 0 mV.

thoroughly, but some evidence suggests a pore-blocking mechanism (Chicchi et al., 1988; Schweitz et al., 1989; Stocker et al., 1991; Werkman et al., 1992). We do not know the mechanism by which HaTx inhibits K^+ channels, but several important clues point to a mechanism other than pore occlusion. The S5-S6 linker does not determine HaTx sensitivity in the same way that it does for the snake and scorpion toxins (Stocker et al., 1991; Gross et al., 1994). Presumably, HaTx interacts with other regions of the K^+ channel. A more subtle clue is provided by the recovery from inhibition seen with HaTx during depolarizing pulses. Given the slow rate of HaTx dissociation at −80 mV (e.g., see Figure 6), partial recovery during a 200 ms depolarizing pulse points to a voltage dependence that is much greater than expected for a pore-blocker. We speculate that HaTx is a gating modifier and is thus very sensitive to the gating state of the channel.

HaTx is unrelated in its sequence to other previously described K^+ channel inhibitors. HaTx is, however, related to grammotoxin (43% identity; see Figure 3), an inhibitor of voltage-activated Ca^{2+} channels isolated from the same spider (Lampe et al., 1992). This finding is very interesting, because HaTx and grammotoxin most likely have similar three-dimensional structures, and therefore, they probably interface with similar surface structures on their target channels. This class of inhibitors should enable us to study a functionally important structure that is shared among voltage-activated cation channels.

Experimental Procedures

K^+ Channel Expression

The Kv2.1 (Frech et al., 1989), *Shaker* H4 (Kamb et al., 1988), Kv3.1

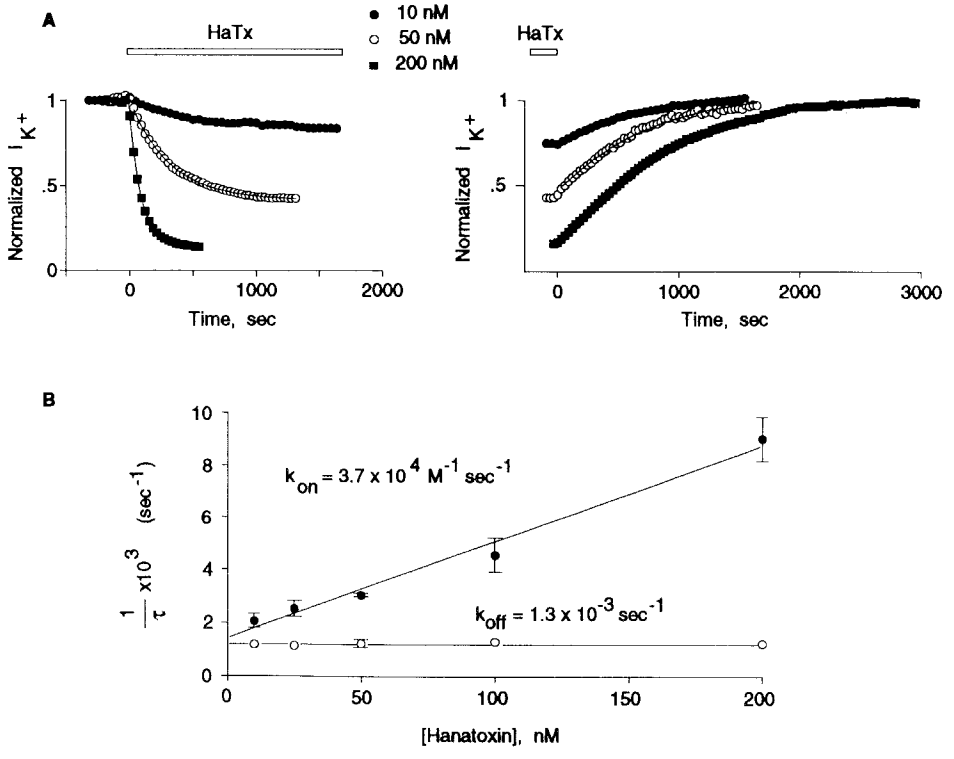

Figure 6. Kinetics of Hanatoxin-Induced Inhibition

(A) Kinetics of inhibition by purified HaTx. Left-hand panel shows onset of inhibition produced by 10, 50, or 200 nM HaTx in three oocytes. The panel on the right shows recovery from inhibition following removal of 10, 50, or 200 nM HaTx in three oocytes.

(B) Plot of $(\tau)^{-1}$ for either onset (closed circles) or recovery (open circles) as a function of HaTx concentration. For onset: n = 4 (200 nM), n = 3 (100 nM), n = 3 (50 nM), n = 3 (25 nM), and n = 3 (10 nM). For recovery: n = 4 (200 nM), n = 3 (100 nM), n = 3 (50 nM), n = 2 (25 nM), and n = 1 (10 nM). The linear fit to the data for onset of inhibition corresponds to $1/\tau = k_{on}[HaTx] + k_{off}$, with $k_{on} = 3.7 \times 10^4\ M^{-1}s^{-1}$ and k_{off} (y intercept) $= 1.4 \times 10^{-3}\ s^{-1}$ (r = 0.99). The mean recovery time constant was 770 ± 23 s ($k_{off} = 1.3 \times 10^{-3} \pm 3.9 \times 10^{-5}\ s^{-1}$). Error bars, SEM.

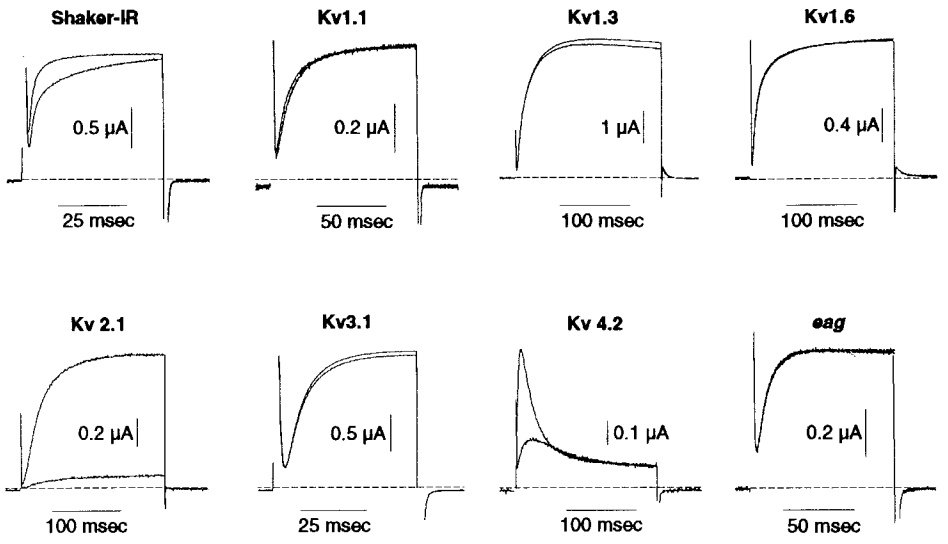

Figure 7. Effect of 500 nM Hanatoxin on Various Voltage-Activated K^+ Channels

All channels were expressed in Xenopus oocytes by injection of cRNA. Mean (± SEM) values for the ratio of current in the presence of 500 nM HaTx to current in control (I/I_o) are as follows: *Shaker*-IR, 0.89 ± 0.012 (n = 5); Kv1.1, 1.02 ± 0.011 (n = 3); Kv1.3, 0.98 ± 0.0097 (n = 3); Kv1.6, 0.98 ± 0.0084 (n = 6); Kv3.1, 0.93 ± 0.014 (n = 4); Kv4.2, 0.27 ± 0.021 (n = 3); and *eag*, 0.97 ± 0.024 (n = 4). For channels that did not inactivate significantly during depolarizations of ≤200 ms, isochronal current measurements were made where the current in control solution had reached steady-state. For Kv4.2, current was measured where the current in control solution reached its peak. All channels were activated by depolarization to 0 mV from a holding potential of either −70 mV (Kv1.3 and Kv1.6) or −80 mV (all others). For Kv1.3, the top trace was recorded in the presence of HaTx and the bottom trace in control solution. For Kv3.1, the top trace was recorded in control solution and the bottom trace in the presence of HaTx.

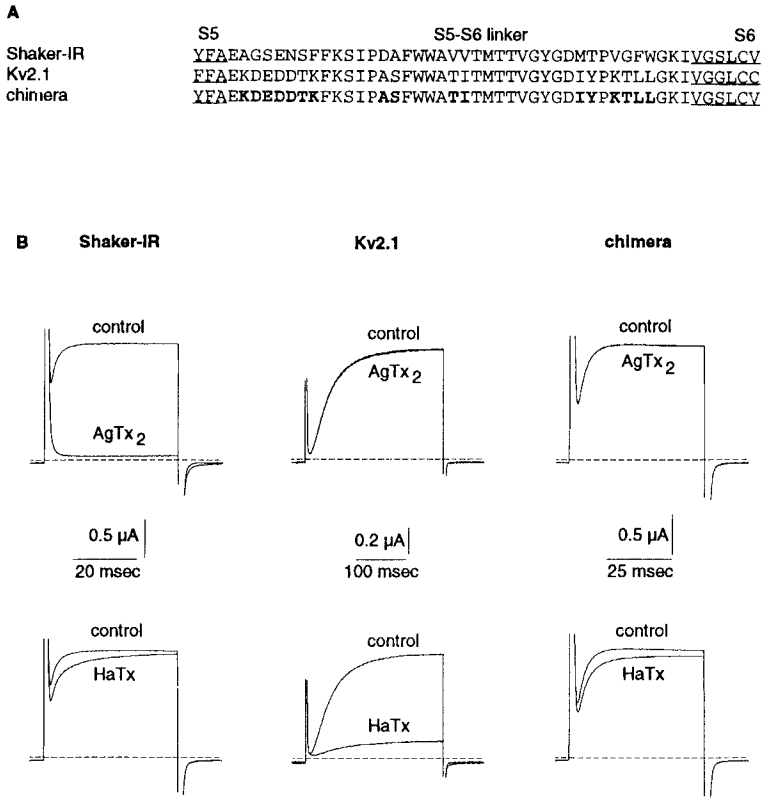

Figure 8. The S5-S6 Linker Does Not Determine Sensitivity to Hanatoxin

(A) Amino acid sequence of S5-S6 linker regions of the *Shaker*-IR, Kv2.1, and chimera K^+ channels. The chimera is a *Shaker* K^+ channel that contains the S5-S6 linker region of Kv2.1. Boldface residues in the chimera indicate positions where it differs from the wild-type *Shaker* channel.

(B) $AgTx_2$ and HaTx sensitivities of the *Shaker*-IR, Kv2.1, and chimera K^+ channels. In all cases, the concentration of $AgTx_2$ was 1 μM, and that of HaTx was 400 nM. $AgTx_2$ and HaTx sensitivities are shown for the same oocyte. Mean (± SEM) values for the ratio of current in the presence of toxin to current in control (I/I_o) are as follows: for *Shaker*-IR, $AgTx_2$, 0.02 (n = 1), HaTx 0.87 ± 0.01 (n = 3); for Kv2.1, $AgTx_2$, 1.01 ± 0.007 (n = 3), HaTx 0.096 ± 0.011 (n = 6); and for chimera, $AgTx_2$, 1.03 ± 0.018 (n = 3), HaTx 0.88 ± 0.013 (n = 6). For all channels, isochronal current measurements were made where the current in control solution had reached steady-state.

(mKv3.1b; Grissmer et al., 1992), and Kv4.2 (rShal; Baldwin et al., 1991) K^+ channel genes were in a Bluescript vector. The Kv1.1 (RCK1; Stühmer et al., 1989) K^+ channel gene was in pGEM-3z, and the Kv1.3 (KV3; Swanson et al., 1990) and Kv1.6 (KV2; Swanson et al., 1990) K^+ channel genes were in pGEM-9zf(−). The *eag* K^+ channel gene was in pGEM-HE (Warmke et al., 1991). The Kv2.1-, Kv1.3-, Kv1.6-, *eag*-, and Kv4.2-bearing plasmids were linearized with NotI. The Kv1.1 K^+ channel plasmid was linearized with PstI, whereas the *Shaker* H4 K^+ channel plasmid was linearized with HindIII. The *Shaker* H4 channel was modified by deleting amino acids 6–46 to remove fast inactivation (Hoshi et al., 1990). The Kv3.1 plasmid was linearized with SacI. All cDNA clones were transcribed using T7 RNA polymerase, except for Kv3.1, which was transcribed using T3 RNA polymerase. cRNA was injected into Xenopus oocytes 16–48 hr prior to electrophysiological recordings.

Electrophysiological Recording

Oocyte membrane potential was controlled using an Axoclamp-2A two-electrode voltage clamp (Axon Instruments). Data were filtered at 2 kHz using an 8-pole Bessel filter and sampled at 3–17 kHz. Microelectrode resistance was 0.3 to 1 MΩ when filled with 3 M KCl. Oocytes were bathed in an ND96 solution containing 0.3 mM $CaCl_2$, 1 mM $MgCl_2$, 2 mM KCl, 96 mM NaCl, and 5 mM HEPES (pH 7.6) with NaOH. Oocytes under voltage clamp were studied in a 100 μl recording chamber that was perfused with ND96 flowing from one of several reservoirs. The entire perfusion system (reservoir, lines, and recording chamber) was fabricated from borosilicate glass, except for two small junctions made using silicon tubing and a low volume Teflon switching valve. The rate of exchange between two solutions was studied using solutions with different KCl concentrations and found to be about 95% complete within 20 s. All reported current measurements were made at 0 mV without leak subtraction in oocytes with less than −40 nA holding current at −80 mV. All experiments were carried out at room temperature (~22°C).

Hanatoxin Biochemistry

Venom from G. spatulata spiders was purchased from Spider Pharm (Feasterville, PA). Venom was diluted 10-fold into 0.1% trifluoroacetic acid (TFA), 10% acetonitrile in H_20, clarified by centrifugation, and filtered through 0.2 μm acrodisc filters (Gelman Sciences, Ann Arbor, MI). The resulting supernatant was fractionated in two steps using reverse-phase high performance liquid chromatography (HPLC), using a Beckman analytical gradient HPLC with either C-8 reverse-phase 5 μm 300 Å or C-18 reverse-phase 5 μm 80 Å columns. Separation and gradient conditions are detailed in the legends to Figures 2 and 4. Mass spectrometric analysis was performed on a VG analytical MALDI-TOF spectrometer. Automated microsequencing was done using an Applied Biosystems 477A protein sequencer after derivatization of cysteine residues with 4-vinylpyridine. The first 33 residues were identified by continuous sequencing from the N terminus. To identify the remaining C terminal residues, a sample of native HaTx was digested with Lys-C (which cleaves after lysine). The resulting fragments were separated by HPLC, and their molecular weights were determined by mass spectrometry. Only one peptide had a molecular weight (1202 KDa) that could not be correlated to the list of peptides generated from known sequence data on the first 33 residues. This peptide was sequenced and found to be YCAWDFTFS, allowing identification of residues 34 and 35 as F and S, respectively. Amino acid analysis was done using an Applied Biosystems 420A Derivatizer and a 130A separation system. Concentrations of HaTx were determined by amino acid analysis.

Production of Recombinant Hanatoxin

An HaTx gene was synthesized using two oligonucleotide duplexes, ligated into pMal (New England Biolabs; Riggs, 1994) using SalI and HindIII restriction sites, and confirmed by sequencing (Sanger et al., 1977). The sense strand was as follows: 5′-TGGACATTGAGGGTATGGAGTGCAGGTACCTCTTCGGGGGGTGCAAGACCACCGCCGACTGCTGCAAGCACCTCGGGTGCAAGTTCAGGGACAAGTACTGCGCCTGGGACTTCACCTTCAGCTAGA-3′. Protein expression was carried out in a DH5αF′ strain of E. coli, in the presence of 500 μM isopropylthiogalctopyranoside at 26°C. Periplasmic protein was harvested by osmotic shock as previously described (Riggs, 1994). The malE–$HaTx_1$ fusion protein was purified from the osmotic shock solution, using amylose resin (New England Biolabs) chromatography. Fractions containing fusion protein were dialyzed against 1 mM Tris–Cl (pH 7.4). The malE–$HaTx_1$ fusion protein (final concentration ≈ 1 mg/ml) was incubated in a solution containing 40% acetic acid, 5% TFA, and 300 mM cyanogen bromide overnight at 22°C in the dark. $HaTx_1$ was initially separated from other fragments of malE using SP sephadex (C-25) chromatography, where $HaTx_1$ eluted around pH 8. The active fold of $HaTx_1$ was then purified by HPLC as shown in Figure 4.

Chimera Construction

A BglII-XmaI fragment that contained the coding region of the S5-S6 linker from Kv2.1 (see Figure 8A) was constructed using the polymerase chain reaction. To construct the chimera, this fragment was substituted for the original corresponding fragment in *Shaker*-IR cDNA and sequenced by dideoxy sequencing (Sanger et al., 1977).

Acknowledgments

We thank J. Rush, C. Miller, R. A. Lampe, K. Rosen, M. E. Adams, Z. Lu, C.-S. Park, A. Gross, P. Hidalgo, and R. Ranganathan for helpful discussions. The work was supported by a grant (GM43949) from the National Institutes of Health.

The costs of publication of this article were defrayed in part by the payment of page charges. This article must therefore be hereby marked *"advertisement"* in accordance with 18 USC Section 1734 solely to indicate this fact.

Received May 11, 1995; revised July 7, 1995.

References

Anderson, C.S., MacKinnon, R., Smith, C., and Miller, C. (1988). Charybdotoxin block of single Ca^{2+}-activated K^+ channels. J. Gen. Physiol. *91*, 317–333.

Baldwin, T.J., Tsaur, M.-L., Lopez, G.A., Jan, Y.N., and Jan, L.Y. (1991). Characterization of a mammalian cDNA for an inactivating voltage-sensitive K^+ channel. Neuron *7* 471–483.

Benishin, C.G., Sorensen, R.G., Brown, W.E., Krueger, B.K., and Blaustein, M.P. (1988). Four polypeptide components of green mamba venom selectively block certain potassium channels in rat brain synaptosomes. Mol. Pharmacol. *34*, 152–159.

Billingham, M.E.J., Morley, J., Hanson, J.M., Shipolini, R.A., and Vernon, C.A. (1973). An anti-inflammatory peptide from bee venom. Nature *245*, 163–164.

Blatz, A.L., and Magleby, K.L. (1986). Single apamin-blocked Ca-activated K^+ channels of small conductance in cultured rat skeletal muscle. Nature *323*, 718–720.

Bontems, F., Roumestand, C., Boyot, P., Gilquin, B., Doljansky, Y., Menez, A., and Toma, F. (1991a). Three-dimensional structure of natural charybdotoxin in aqueous solution by 1H-NMR. Eur. J. Biochem. *196*, 19–28.

Bontems, F., Roumestand, C., Gilquin, B., Menez, A., and Toma, F. (1991b). Refined structure of charybdotoxin: common motifs in scorpion toxins and insect defensins. Science *254*, 1521–1523.

Carbone, E., Prestipino, G., Spadavecchia, L., Franciolini, F., and Possani, L.D. (1987). Blocking of the squid axon K^+ channel by noxiustoxin: a toxin from the venom of the scorpion *Centruroides noxius*. Pflügers Arch. *408*, 423–431.

Chicchi, G.G., Gimenez-Gallego, G., Ber, E., Garcia, M.L., Winquist, R., and Cascieri, M.A. (1988). Purification and characterization of a unique, potent inhibitor of apamin binding from *Leiurus quinquestriatus hebraeus* venom. J. Biol. Chem. *263*, 10192–10197.

Crest, M., Jacquet, G., Gola, M., Zerrouk, H., Benslimane, A., Rochat, H., Mansuelle, P., and Martin-Eauclaire, M.-F. (1992). Kaliotoxin, a novel peptidyl inhibitor of neuronal BK-type Ca^{2+}-activated K^+ channels characterized from *Androctonus mauretanicus mauretanicus* venom. J. Biol. Chem. *267*, 1640–1647.

Foray, M.-F., Lancelin, J.-M., Hollecker, M., and Marion, D. (1993). Sequence-specific 1H-NMR assignment and secondary structure of black mamba dendrotoxin-I, a highly selective blocker of voltage-gated potassium channels. Eur. J. Biochem. *211*, 813–820.

Frech, G.C., VanDongen, A.M.J., Schuster, G., Brown, A.M., and Joho, R.H. (1989). A novel potassium channel with delayed rectifier properties isolated from rat brain by expression cloning. Nature *340*, 642–645.

Galvez, A., Gimenez-Gallego, G., Reuben, J.P., Roy-Contancin, L., Feigenbaum, P., Kaczorowski, G.J., and Garcia, M.L. (1990). Purification and characterization of a unique, potent, peptidyl probe for the high conductance calcium-activated potassium channel from venom of the scorpion *Buthus tamulus*. J. Biol. Chem. *265*, 11083–11090.

Garcia, M.L., Garcia-Calvo, M., Hidalgo, P., Lee, A.W., and MacKinnon, R. (1994). Purification and characterization of three inhibitors of voltage-dependent K^+ channels from *Leiurus quinquestriatus* var. *hebraeus* venom. Biochem. *33*, 6834–6839.

Garcia-Calvo, M., Leonard, R.J., Novick, J., Stevens, S.P., Schmalhofer, W., Kaczorowski, G.J., and Garcia, M.L. (1993). Purification, characterization, and biosynthesis of margatoxin, a component of *Centruroides margaritatus* venom that selectively inhibits voltage-dependent potassium channels. J. Biol. Chem. *268*, 18866–18874.

Goldstein, S.A.N., Pheasant, D.J., and Miller, C. (1994). The charybdotoxin receptor of a *Shaker* K^+ channel: Peptide and channel residues mediating molecular recognition. Neuron *12*, 1377–1388.

Grissmer, S., Ghanshan, S., Dethlefs, B., McPherson, J.D., Wasmuth, J.J., Gutman, G.A., Cahalan, M.D., and Chandy, K.G. (1992). The *Shaw*-related potassium channel gene, Kv3.1, on human chromosome 11, encodes the type I K^+ channel in T cells. J. Biol. Chem. *267*, 20971–20979.

Grissmer, S., Nguyen, A.N., Aiyar, J., Hanson, D.C., Mather, R.J., Gutman, G.A., Karmilowicz, M.J., Auperin, D.D., and Chandy, K.G. (1994). Pharmacological characterization of five cloned voltage-gated K^+ channels, types 1.1, 1.2, 1.3, 1.5 and 3.1 stably expressed in mammalian cell lines. Mol. Pharmacol. *45*, 1227–1234.

Gross, E., and Witkop, B. (1962). Nonenzymatic cleavage of peptide bonds: the methionine residues in bovine pancreatic ribonuclease. J. Biol. Chem. *237*, 1856–1860.

Gross, A., Abramson, T., and MacKinnon, R. (1994). Transfer of the scorpion toxin receptor to an insensitive channel. Neuron *13*, 961–966.

Gutman, G.A., and Chandy, K.G. (1993). Nomenclature of mammalian voltage-dependent potassium channel genes. Semin. Neurosci. *5*, 101–106.

Halliwell, J.V., Othman, I.B., Pelchen-Matthews, A., and Dolly, J.O. (1986). Central actions of dendrotoxin: selective reduction of a transient K^+ conductance in hippocampus and binding to localized acceptors. Proc. Natl. Acad. Sci. USA *83*, 493–497.

Hartmann, H.A., Kirsch, G.E., Drewe, J.A., Joho, R.H., and Brown, A.M. (1991). Exchange of conduction pathways between two related K^+ channels. Science *251*, 942–944.

Harvey, A.L., and Anderson, A.J. (1985). Dendrotoxins: snake toxins that block potassium channels and facilitate neurotransmitter release. Pharmacol. Ther. *31*, 33–55.

Harvey, A.L., and Karlsson, E. (1980). Dendrotoxin from the venom of the green mamba, *Dendroaspis angusticeps*. A neurotoxin that enhances acetylcholine release of neuromuscular junctions. Naunyn Schmiedebergs Arch. Pharmacol. *312*, 1–6.

Haux, P., Sawerthal, H., and Habermann, E. (1967). Sequenzanalyse des Bienengift-Neurotoxins (Apamin) aus seinen tryptischen und chymotryptischen Spatstücken. Hoppe Seylers Z. Physiol. Chem. *348*, 737–738.

Hildago, P., and MacKinnon, R. (1995). Revealing the architecture of a K^+ channel pore through mutant cycles with a peptide inhibitor. Science *268*, 307–310.

Hoshi, T., Zagotta, W.N., and Aldrich, R.W. (1990). Biophysical and molecular mechanisms of *Shaker* potassium channel inactivation. Science *250*, 533–568.

Hurst, R.S., Busch, A.E., Kavanaugh, M.P., Osborne, P.B., North, R.A., and Adelman, J.P. (1991). Identification of amino acid residues involved in dendrotoxin block of rat voltage-dependent potassium channels. Mol. Pharmacol. *40*, 572–576.

Hwang, P.M., Fotuhi, M., Bredt, D.S., Cunningham, A.M., and Snyder, S.H. (1993). Contrasting immunohistochemical localizations in rat brain of two novel K^+ channels of the *Shab* subfamily. J. Neurosci. *13*, 1568–1576.

Johnson, B.A., and Sugg, E.E. (1992). Determination of the three-dimensional structure of iberiotoxin in solution by 1H-nuclear magnetic resonance spectroscopy. Biochem. *31*, 8151–8159.

Joubert, F.J., and Taljaard, N. (1980). The amino acid sequences of two proteinase inhibitor homologues from *Dendroaspis angusticeps* venom. Hoppe Seylers Z. Physiol. Chem. *361*, 661–674.

Kamb, A., Tseng-Crank, J., and Tanouye, M.A. (1988). Multiple products of the Drosophila *Shaker* gene may contribute to potassium channel diversity. Neuron *1*, 421–430.

Kirsch, G.E., Drewe, J.A., Verma, S., Brown, A.M., and Joho, R.H. (1991). Electrophysiological characterization of a new member of the RCK family of rat brain K^+ channels. FEBS Lett. *278*, 55–60.

Krezel, A., Kasibhatla, C., Hidalgo, P., MacKinnon, R., and Wagner, G. (1995). Solution structure of the potassium channel inhibitor agitoxin 2: caliper for probing channel geometry. Protein Sci. *4*, 1478–1489.

Kumar, N.V., Wemmer, D.E., and Kallenbach, N.R. (1988). Structure of P401 (mast cell degranulating peptide) in solution. Biophys. Chem. *31*, 113–119.

Lambert, P., Kuroda, H., Chino, N., Watanabe, T.X., Kimura, T., and Sakakibara, S. (1990). Solution synthesis of charybdotoxin (ChTX), a K^+ channel blocker. Biochem. Biophys. Res. Commun. *170*, 684–690.

Lampe, R.A., Defeo, P.A., Davison, M.D., Young, J., Herman, J.L., Spreen, R.C., Horn, M.B., Mangano, T.J., and Keith, R.A. (1993). Isolation and pharmacological characterization of ω-conotoxin SIA, a novel peptide inhibitor of neuronal voltage-sensitive calcium channel responses. Mol. Pharmacol. *44*, 451–460.

Lucchesi, K., Ravindran, A., Young, H., and Moczydlowski, E. (1989). Analysis of the blocking activity of charybdotoxin homologs and iodinated derivatives against Ca^{2+}-activated K^+ channels. J. Memb. Biol. *109*, 269–281.

MacKinnon, R., and Miller, C. (1988). Mechanism of charybdotoxin block of the high-conductance, Ca^{2+}-activated K^+ channel. J. Gen. Physiol. *91*, 335–349.

MacKinnon, R., and Miller, C. (1989). Mutant potassium channels with altered binding of charybdotoxin, a pore-blocking peptide inhibitor. Science *245*, 1382–1385.

MacKinnon, R., Heginbotham, L., and Abramson, T. (1990). Mapping the receptor site for charybdotoxin, a pore-blocking potassium channel inhibitor. Neuron *5*, 767–771.

MacKinnon, R. (1991). Determination of the subunit stoichiometry of a voltage-activated potassium channel. Nature *350*, 232–235.

MacKinnon, R., Aldrich, R.W., and Lee, A.W. (1993). Functional stoichiometry of shaker potassium channel inactivation. Science *262*, 757–759.

Miller, C. (1988). Competition for block of a Ca^{2+}-activated K^+ channel by Charybdotoxin and tetraethylammonium. Neuron *1*, 1003–1006.

Miller, C., Moczydlowski, E., Latorre, R., and Phillips, M. (1985). Charybdotoxin, a protein inhibitor of single Ca^{2+}-activated K^+ channels from mammalian skeletal muscle. Nature *313*, 316–318.

Park, C.-S., and Miller, C. (1992). Interaction of charybdotoxin with permeant ions inside the pore of a K^+ channel. Neuron *9*, 307–313.

Pease, J.H.B., and Wemmer, D.E. (1988). Solution structure of apamin determined by nuclear magnetic resonance and distance geometry. Biochem. *27*, 8491–8498.

Penner, R., Petersen, M., Pierau, F.-K., and Dreyer, F. (1986). Dendrotoxin: a selective blocker of a non-inactivating potassium current in guinea-pig dorsal root ganglion neurones. Pflügers Arch. *407*, 365–369.

Possani, L.D., Martin, B.M., and Svendsen, I.B. (1982). The primary

structure of noxiustoxin: a K^+ channel blocking peptide, purified from the venom of the scorpion *Centruroides noxius hoffmann*. Carlsberg Res. Commun. *47*, 285–289.

Reger, W.G., and Mintz, I.M. (1994). Participation of multiple calcium channel types in transmission at single climbing fiber to Purkinje cell synapses. Neuron *12*, 605–613.

Riggs, P. (1994). Expression and purification of maltose-binding protein fusions. In Current Protocols in Molecular Biology, F. Ausubel, et al., eds. (Current Protocols Inc.), unit 16.6.

Robitaille, R., Garcia, M., Kaczorowski, G.J., and Charlton, M.P. (1993). Functional colocalization of calcium and calcium-gated potassium channels in control of transmitter release. Neuron *11*, 645–655.

Sanger, F., Nicklen, S., and Coulson, A.R. (1977). DNA sequencing with chain-terminating inhibitors. Proc. Natl. Acad. Sci. USA *74*, 5463–5467.

Schweitz, H., Bidard, J.-N., Maes, P., and Lazdunski, M. (1989). Charybdotoxin is a new member of the K^+ channel toxin family that includes dendrotoxin I and mast cell degranulating peptide. Biochemistry *28*, 9708–9714.

Shipolini, R.A., Bradbury, A.F., Callewaet, G.L., and Vernon, C.A. (1967). The structure of apamin. Chem. Commun. 679–680.

Skarzynski, T. (1992). Crystal structure of α-Dendrotoxin from the greem mamba venom and its comparison with the structure of bovine pancreatic trypsin inhibitor. J. Mol. Biol. *224*, 671–683.

Smith, C., Phillips, M., and Miller, C. (1986). Purification of charybdotoxin, a specific inhibitor of the high-conductance Ca^{2+}-activated K^+ channels. J. Biol. Chem. *261*, 14607–14613.

Stampe, P., Kolmakova-Partensky, L., and Miller, C. (1994). Intimations of K^+ channel structure from a complete functional map of the molecular surface of charybdotoxin. Biochemistry. *33*, 443–450.

Stansfeld, C.E., Marsh, S.J., Halliwell, J.V., and Brown, D.A. (1986). 4-Aminopyridine and dendrotoxin induce repetitive firing in rat visceral sensory neurones by blocking a slowly inactivating outward current. Neurosci. Lett. *64*, 299–304.

Stocker, M., and Miller, C. (1994). Electrostatic distance geometry in a K^+ channel vestibule. Proc. Natl. Acad. Sci. USA *91*, 9509–9513.

Stocker, M., Pongs, O., Hoth, M., Heinemann, S.H., Stühmer, W., Schröter, K.-H., and Ruppersberg, J.P. (1991). Swapping of functional domains in voltage-gated K^+ channels. Proc. R. Soc. Lond. B *245*, 101–107.

Strydom, D.J. (1972). Snake venom toxins: the amino acid sequences of two toxins from *Dendroaspis polylepis polylepis* (black mamba). venom. J. Biol. Chem. *247*, 4029–4042.

Strydom, D.J. (1973). Protease inhibitors as snake venom toxins. Nature New Biol. *243*, 88–89.

Stühmer, W., Ruppersberg, J.P., Schröter, K.H., Sakmann, B., Stocker, M., Giese, K.P., Perschke, A., Baumann, A., and Pongs, O. (1989). Molecular basis of functional diversity of voltage-gated potassium channels in mammalian brain. EMBO J. *8*, 3235–3244.

Swanson, R., Marshall, J., Smith, J.S., Williams, J.B., Boyle, M.B., Folander, K., Luneau, C.J., Antanavage, J., Oliva, C., Buhrow, S.A., et al. (1990). Cloning and expression of cDNA and genomic clones encoding three delayed rectifier potassium channels in rat brain. Neuron *4*, 929–939.

Trimmer, J.S. (1991). Immunological identification and characterization of a delayed rectifier K^+ channel polypeptide in rat brain. Proc. Natl. Acad. Sci. USA *88*, 10764–10768.

Warmke, J., Drysdale, R., and Ganetzky, B. (1991). A distinct potassium channel polypeptide encoded by the *Drosphila eag* locus. Science *252*, 1560–1562.

Werkman, T.R., Kawamura, T., Yokoyama, S., Higashida, H., and Rogawski, M.A. (1992). Charybdotoxin, dendrotoxin, and mast cell degranulating peptide block the voltage-activated K^+ current of fibroblast cells stably transfected with NGK1 (Kv1.2) K^+ channel complementary DNA. Neuroscience *50*, 935–946.

Werkman, T.R., Gustafson, T.A., Rogowski, R.S., Blaustein, M.P., and Rogawski, M.A. (1993). Tityustoxin-K-α, a structurally novel and highly potent K^+ channel peptide toxin, interacts with the α-dendrotoxin binding site on the cloned Kv1.2 K^+ channel. Mol. Pharmacol. *44*, 430–436.

Yellen, G., Jurman, M.E., Abramson, R., and MacKinnon, R. (1991). Mutations affecting internal TEA blockade identify the probable pore-forming region of a K^+ channel. Science *251*, 939–942.

Yool, A.J., and Schwarz, T.L. (1991). Alteration of ionic selectivity of a K^+ channel by mutation of the H5 region. Nature *349*, 700–704.